IOSR Journal of Applied Chemistry (IOSR-JAC)
e-ISSN: 2278-5736.Volume 18, Issue 12 Ser. I (December. 2025), PP 26-36
www.iosrjournals.org

Determination Of The Acidity Or Basicity Constants Of Tyramine In The Ground And Excited States

Papa Adama Ndione[1,2], Amadou Sarr Gning[3], Coumba Gueye[1], Diéry Diouf[1], Moussa Mbaye[1], Khémesse Kital[1], Olivier Maurice Ali Mbaye[1], Lamine Cissé[1], François Delattre[4], Atanasse Coly[1], Mame Diabou Gaye-Seye[1], Alphonse Tine[1]

Laboratoire De Photochimie Et D'analyse (Lpa), Faculté Des Sciences Et Techniques, Université Cheikh Anta Diop De Dakar, Sénégal. B.P 5005
Laboratoire National De Contrôle Des Médicaments, Dakar, Sénégal
Laboratoire De Chimie Physique Organique Et D'analyses Environnementales (Lcpoae), Université Cheikh Anta Diop, Dakar, Sénégal
Laboratoire De Synthèse Organique Et Environnement, Ea2599, Université Du Littoral Côte D'opale, 145 Avenue Maurice Schumann, Bp 59140 Dunkerque, France

Abstract
Tyramine (4-[2-aminoethyl]phenol) belongs to the trace amines, a family of endogenously synthesized compounds present in the body at nanomolar concentrations. The objective of this work is to determine the acidity and basicity constants of tyramine in the ground and excited states, with the aim of evaluating its behavior in different environments. First, the acidity constant (Ka) in the ground state was determined by varying the percentage of acidic and basic species as a function of pH, then using the Henderson-Hasselbalch formula. Second, the acidity constant in the excited state (Ka) was determined using the Förster cycle. Using the first method, an average $pK_A(S_0)$ value of 10.55 was found; the second method yielded a $pK_A(S_0)$ value of 10.61. The FÖRSTER cycle allowed the calculation of a $pK_A^*(S_1)$ value of 4.7. Based on the results, tyramine tends to be basic in its ground state, and rather acidic in its excited state.*

Keywords *: Tyramine, Absorption, Acidity constants of the ground (pKa) and excited (pKa*) states, Förster cycle*

Date of Submission: 05-12-2025 Date of Acceptance: 15-12-2025

I. Introduction

Tyramine is the most prevalent biogenic amine in food products. It is produced by microorganisms during the decarboxylation of tyrosine [1, 2]. Fermented foods and beverages, such as cheeses, fermented fish, soy sauces, wines, and others, likely contain some level of tyramine [3]. Tyramine has been declared a biological hazard for food and beverages by the European Food Safety Authority (EFSA) and the Food and Agriculture Organization of the United Nations (FAO) [4,5]. However, tyramine is not present in very fresh foods, but appears and increases during storage due to microbial decarboxylation of the amino acid tyrosine. The tyramine content of foods is not specifically regulated by law, although it is strongly suspected that it contributes to increased histamine concentrations in the human body (histamine concentration limits in some foods have been set by the European Union) [6, 7]. Moreover, tyramine is the predominant biogenic amine in some foods, and its maximum content in some products is regulated by the corresponding Codex Alimentarius of some countries [8]. The determination of tyramine in foods presents similar difficulties to the analysis of other biological substances: the complexity of the sample matrix and its low concentration. Therefore, it is almost inevitable to carry out a preliminary extraction to eliminate interferences, concentrate the samples and apply an instrumental separation technique such as thin-layer chromatography, gas chromatography, capillary electrophoresis or high-resolution liquid chromatography. These methodologies have been described in previous articles [9, 10]. All these methods are very effective, but they require a long analysis and skilled personnel. Therefore, they are generally used when several biogenic amines need to be determined. Rapid response methods are needed to quickly detect high concentrations of tyramine in food to effectively protect consumers, workers and producers. Our previous work has quantified the level of tyramine in some fish products by the spectrofluorimetric method knowing that it is naturally fluorescent [11].

Therefore, it is necessary to study the physical and chemical properties of tyramine as a function of electronic states to understand chemical reactions and to deduce the acidity or basicity constants in the ground and excited states.

It has long been known that the fluorescence spectrum of certain phenols, acids, and aromatic amines in aqueous solution depends on pH. A simple explanation for this phenomenon could be that it depends on whether the acidic or basic form of the pair is excited.

The electronic structure of a molecule determines its physical and chemical properties. The absorption of a photon with an energy equal to the quantum level difference leads to the excitation of an electron from the ground state to the first excited singlet state, $S_0 > S_1$. The change in electron distribution can lead to chemical reactions in the excited state. The excited state has a relatively short lifetime, from 10^{-6} to 10^{-11} seconds, making it difficult to measure the properties of the excited state. Excited-state decay can occur through radiative processes, photon ejection, or nonradiative energy transfer. Radiative fluorescence, $S_1 > S_0$, is an effective method for measuring excited-state properties.

In this experiment, we consider the interaction of a fluorophore, tyramine, with its environment and determine its dissociation constant in the ground singlet state and in the first excited state. Tyramine can be an acid or a base in aqueous solution.

The dissociation of tyramine varies depending on the molecule's electronic state.

II. Materials And Methods

Reagent and Solvents

Tyramine (97%, w/w) was purchased from Sigma-Aldrich and used without further purification. The tyramine stock standard solution (10^{-2} M) was freshly prepared by dissolving the compound in water. Serial dilutions were performed to obtain working standard solutions.

Apparatus

The electronic absorption spectra of tryptamine were obtained in several solvents at room temperature using a UV-visible spectrophotometer (Cary 100 Spectrophotometer). Statistical analysis of the data was performed using OriginPro 8.5.1 software.

III. Results And Discussions

Preliminary UV-vis Absorption Spectrophotometry Study of Tyramine

In this section, the effect of pH on the wavelength shifts of the UV-visible absorption spectra of tyramine was investigated. These wavelength shifts allowed us to determine the acidity constants of the ground (pK_A) and excited (pK_A^*) states using the Förster cycle.

Determination of the Absorption Spectrum of Tyramine in Water

The absorption spectrum of tyramine in water is shown in Figure 1. This spectrum includes two absorption bands with peaks at 222 nm and 278 nm, respectively. We applied Beer Lambert's law to determine the molar extinction coefficients (εmax) corresponding to these absorption maxima. With the concentration of 10-5 M and a step of 1 cm we therefore find respectively εmax = 16149 $M^{-1}.cm^{-1}$ for the peak at 222 nm and εmax = 14091 $M^{-1}.cm^{-1}$ for that of 278 nm. These molar extinction coefficients (εmax) being greater than 104 $M^{-1}.cm^{-1}$ show that these various electronic transitions are all of the π-π* type.

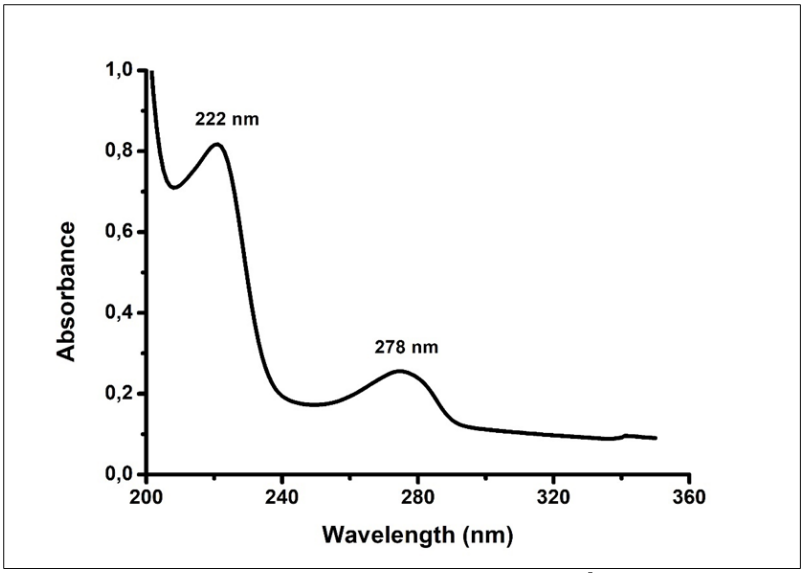

Figure 1: Absorption spectrum of tyramine (10^{-5} M) in water

Effect of pH on Tyramine Absorption Spectra

Figure 2 shows the absorption spectra of tyramine in aqueous media at different pHs. It can be seen that the molecule's absorption bands are highly dependent on the medium. In acidic media, the absorption spectrum of tyramine exhibits two bands, one more intense with a peak at 205 nm and the other at 258 nm. Similarly, in alkaline media, the absorption spectrum of tyramine also exhibits two bands, one more intense with a peak at 222 nm and the other less intense with a peak at 278 nm.

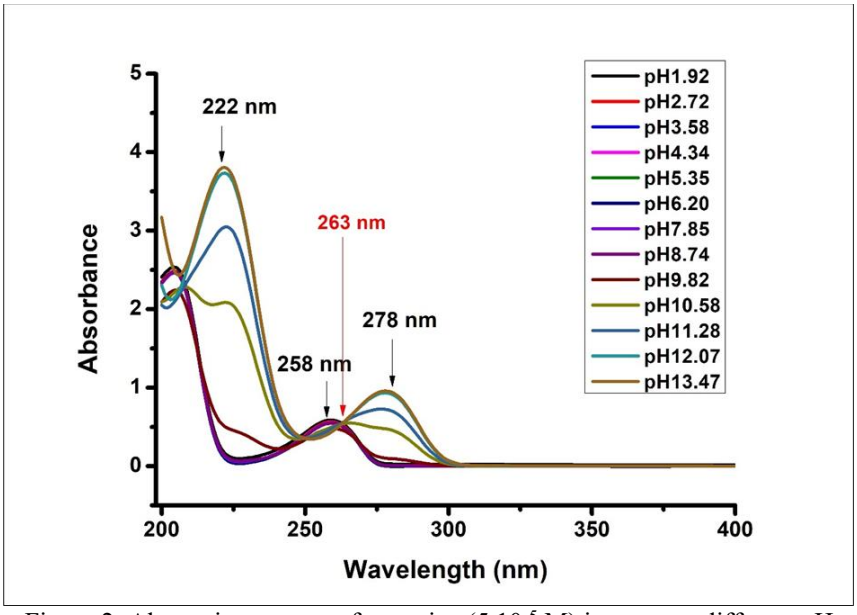

Figure 2: Absorption spectra of tyramine (5.10^{-5} M) in water at different pH

A bathochromic shift of the absorption peak is observed when moving from acidic to basic pH, demonstrating an ionization effect on the alcohol function of tyramine. In addition, the isosbestic point at 263 nm demonstrates the existence of an equilibrium between the acidic ($R-OH$) and basic ($R-O^-$) forms. In an acidic medium, the absorption spectrum, with two peaks at 205 and 258 nm, respectively, corresponds to that of the acidic ($R-OH$) form. However, in an alkaline medium, the spectrum, with two peaks at 222 and 278 nm, respectively, corresponds to the spectra of the basic ($R-O^-$) form. We can therefore write the following equilibrium (Figure 3) :

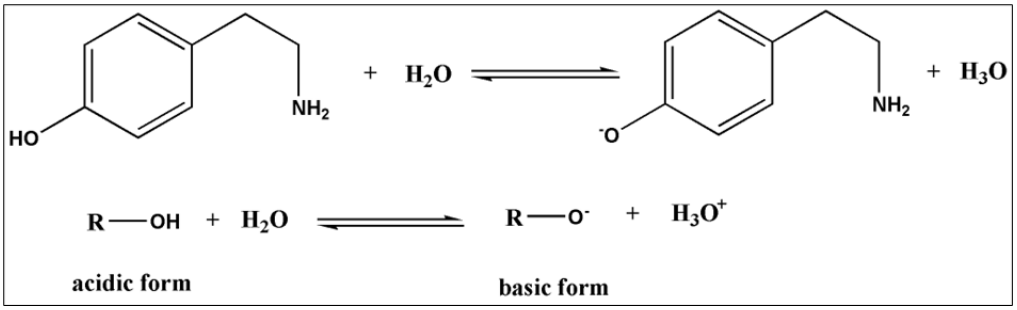

Figure 3 : Acid-base equilibrium of tyramine in water

Determination of acidity constants in the ground (pK_A) and excitatory (pK_A^*) states

Absorption spectra have two forms depending on the pH of the medium. In acidic media, we have the absorption spectra of the acidic form (R-OH) and in basic media, those of the basic form ($R-O^-$).

To determine the le pK_A in the ground state, the spectra in basic media were used. In reality, the variation in absorbance as a function of pH is not quantifiable in acidic media because all spectra have the same intensity regardless of the pH in this medium (Figure 2). In all cases, the percentage of the acidic form % [R-OH] and that of the basic form % $[R-O^-]$ or the ratio $\frac{[R-O^-]}{[R-OH]}$ must be known depending on the method used. To calculate the $pK_A(S_0)$ two methods were used on the one hand the percentage of acidic and basic species was varied according to the pH and on the other hand using the Henderson-Hasselbalch formula.

Determination of $pK_A(S_0)$ from the evolution of the percentages of acidic and basic species as a function of pH.

Determination of $pK_A(S_0)$ using the λ_{ab}= 278 nm peak.

In solution, deprotonation of $R-OH$ to $R-O^-$ occurs in part according to the equilibrium :

$$R-OH + H_2O \rightleftarrows R-O^- + H_3O^+$$

If the concentration of the prepared tyramine solution is C_0, in solution we can write :

$$C_0 = [R-OH] + [R-O^-]$$

The absorbance of tyramine in solution can be written as

$A = K_1[R-OH] + K_2[R-O^-]$ according to Beer Lambert's law: (Eq-1)

With $K_1 = \varepsilon_1 l$ and $K_2 = \varepsilon_2 l$

$\varepsilon_1 \; et \; \varepsilon_2$: represent the molar extinction coefficients of the acid form $(R-OH)$ and the basic form $(R-O^-)$ respectively; l represents the optical path pitch (typically 1 cm).

At this length, 278 nm, the absorbance of the acidic form is zero or very negligible compared to that of the basic form. Thus we can write :

$A = K_2[R-O^-]$ (Eq-2)

Assuming total dissociation in a very basic medium (pH max), the concentration ($[R-O^-]$) is equal to C_0. In this case, we can write :

$A_m = K_2C_0$ (Eq-3)

With A_m the maximum absorbance of the basic form $(R-O^-)$.

From the two expressions (Eq-2) and (Eq-3) we can write: $\frac{[R-O^-]}{C_0} = \frac{A}{A_m}$ (Eq-4)

Thus, the percentage of $[R-O^-]$ noted $\%[R-O^-] = \frac{[R-O^-]}{C_0} \times 100 = \frac{A}{A_m} \times 100$ (Eq-5)

From equation (Eq-1) and taking into account the low absorbance of the acid form at wavelength 278 nm, we can write :

$C_0 = [R-OH] + [R-O^-] \Longrightarrow [R-OH] = C_0 - [R-O^-]$ hence

$$\frac{[R-OH]}{C_0} = \frac{C_0-[R-O^-]}{C_0} = \left(1 - \frac{A}{A_m}\right) \quad \text{(Eq-6)}$$

Thus, the percentage of $\%\,[R-OH] = \frac{C-[R-O^-]}{C_0} \times 100 = \left(1 - \frac{A}{A_m}\right) \times 100$ (Eq-7)

Based on the pH values, it is therefore possible to determine the $\%[\,R-O^-$ and $\%[\,R-OH]$ percentages using equations (Eq-5) and (Eq-7) respectively. Absorbances were determined from figure 2.
All results are shown in Table 1.

Table 1: Variation in the percentage of the acidic (a) or basic (b) form as a function of pH

pH	Absorbance	% [R − OH] (a)	% [R − O⁻] (b)
1.92	0.032	96.67	3.33
2.72	0.011	98.85	1.15
3.58	0.003	99.69	0.31
4.34	0.006	99.375	0.625
5.35	0	100	0
6.2	0.001	99.9	0.1
7.85	0.01	98.96	1.04
8.74	0.012	98.75	1.25
9.82	0.102	89.36	10.64
10.58	0.477	50.26	49.74
11.28	0.724	24.51	75.49
12.07	0.934	2.61	97.39
13.47	0.959	0	100

To determine $pK_A(S_0)$, the curves were plotted respectively

$\%\,[R-OH] = f(pH)$ curve (a) and

$\%[R-O^-] = f(pH)$ curve (b)

The intersection of the two curves gives the value of $pK_A(S_0)$ (figure 4).
Measurements give a value of $pK_A(S_0)$ = 10.60.

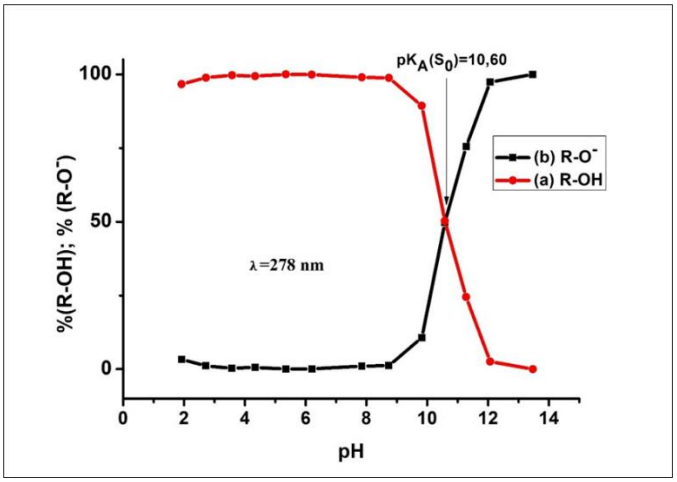

Figure 4: Respective evolutions of $\%[R-OH]$ (curve a) and $\%[R-O^-]$ (curve b) as a function of pH at λ_{ab}= 278 nm

Determination of $pK_A(S_0)$ using the peak λ_{ab}= 222 nm

At this wavelength the absorbance of the acid form is zero if not negligible. We therefore used the same types of calculation to determine the percentages of the two species. Table 2 shows all the results (variation of the acidic species, variation of the basic species and absorbance as a function of pH), using the absorption spectra in Figure 2.

Table 2: Variation in the percentage of the acidic (a) or basic (b) form as a function of pH

pH	Absorbance	% $[R-OH]$ (a)	% $[R-O^-]$ (b)
1.92	0.111	97.09	2.91
2.72	0.096	97.48	2.52
3.58	0.106	97.22	2.78
4.34	0.165	95.67	4.33
5.35	0.101	97.35	2.65
6.2	0.103	97.29	2.71
7.85	0.125	96.72	3.28
8.74	0.135	96.45	3.55
9.82	0.504	86.76	13.24
10.58	2.086	45.21	54.79
11.28	3.047	19.96	80.04
12.07	3.735	1.89	98.11
13.47	3.807	0	100

From this table, the curve showing the variation of the percentage of the acidic form (a) or the basic form (b) as a function of pH is shown (Figure 5).

The intersection of the two curves (a) and (b) gives the $pK_A(S_0)$ value of the acid-base equilibrium at around 10.50.

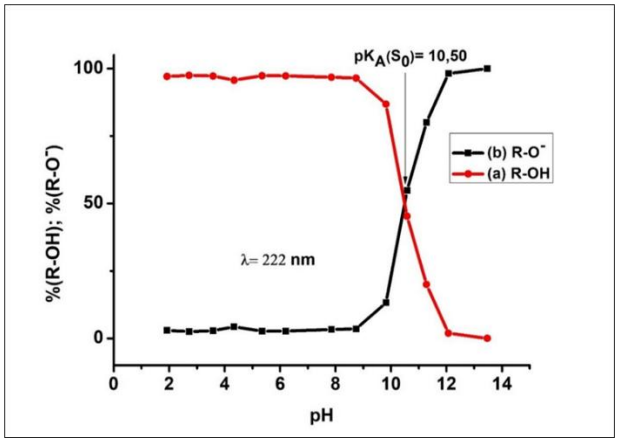

Figure 5: Respective evolutions of $\%\ [R-OH]$ (curve a) and $\%[R-O^-]$ (curve b) as a function of pH at λ_{ab}= 222 nm

Using the two lengths of 278 nm and 222 nm yields $pK_A(S_0)$ values of 10.60 and 10.50, respectively. Thus, the average $pK_A(S_0)$ value is 10.55, which is very close to the value of 10.52 found in the literature [12-14]. Furthermore, this method can be confirmed as highly accurate for determining the acidity and basicity constants in the ground state.
To confirm the accuracy of the previous experiment, the Henderson-Hasselbalch formulation was used.

Determination of $pK_A(S_0)$ from Henderson's relation

Henderson's relation uses the pH formulation of a buffer solution: $pH = pK_A + \log\frac{[Base]}{[Acid]}$; thus the curve of the $pH = f(\log\frac{[Base]}{[Acid]})$ curve is a straight line whose y-intercept gives the pK_A value [15] (Vidal Salgado &Vargas-Hernández, 2014). In our case, the $\frac{[R-O^-]}{[R-OH]}$ ratio is represented by the $\frac{[R-O^-]}{[R-OH]}$ ratio. This ratio is calculated according to the variation in absorbance of the peak under consideration as a function of pH.

Determination of the $pK_A(S_0)$ using the peak λ_{ab}= 278 nm

The principle of this method is to determine the ratio $\frac{[R-O^-]}{[R-OH]}$ as a function of pH. This ratio can be determined from the variation of absorbance with pH using Beer-Lambert's law.

Consider the equilibrium:

$$R-OH + H_2O \rightleftharpoons R-O^- + H_3O^+$$

In this formula, $[R-OH]$ represents the concentration of the acid form and $[R-O^-]$ that of the basic form. $[R-OH]$ and $[R-O^-]$ can therefore be determined for each pH value using absorbances. This can be represented by the equation below:

$$R-OH + H_2O \rightleftharpoons R-O^- + H_3O^+$$

$t = 0$ $\quad C_0 \quad$ 0
$t \neq 0$ $\quad C_0 - x \quad$ x
This shows us $[R-OH] = C_0 - x$ and $[R-O^-] = x$

Using figure 3 and taking into account the additivity of absorbance, we can write for a given pH value
$A = A_1 + A_2$
With $A_1 = K_1[R-OH]$ et $A_2 = K_2[R-O^-]$
K_1 and K_2 represent the same expressions as before.

The total absorbance can therefore be written as: $A = K_1[R-OH] + K_2[R-O^-]$ (Eq-1)

$\Leftrightarrow A = K_1(C_0-x) + K_2 x$
$\Leftrightarrow x = \frac{A-K_1C_0}{K_2-K_1} \quad \Longrightarrow \quad C_0 - x = \frac{K_2C_0-A}{K_2-K_1}$ (Eq-8)
Thus, the $\frac{[R-O^-]}{[R-OH]} = \frac{x}{C_0-x} = \frac{A-K_2C_0}{K_1C_0-A}$ (Eq-9)
The limiting forms can therefore be written as:
$A_{max} = K_2C_0$ corresponding to the basic form (minimal acidic form).
$A_{min} = K_1C_0$ corresponding to the acidic form (minimal basic form).
A= Total absorbance at a given point.
Thus, $\frac{x}{C_0-x} = \frac{A-A_{max}}{A_{min}-A}$ and the relationship (Eq-9) becomes :
$pH = pK_A(S_0) + \log\left(\frac{A-A_{max}}{A_{min}-A}\right)$ (Eq-10)
For any pH value, we therefore determined the ratio $\frac{A-A_{max}}{A_{min}-A}$ then the $\log\left(\frac{A-A_{max}}{A_{min}-A}\right)$ using figure 2.
All the results are grouped in Table 3.

Table 3: pH variation as a function of the ratio of concentrations of the basic form to the acidic form

pH	Absorbance	$\frac{A-A_{max}}{A_{min}-A}$	$\log\left(\frac{A-A_{max}}{A_{min}-A}\right)$
1.92	0.032	29.90	1.47
2.72	0.011	94.8	1.98
3.58	0.003	478	2.68
4.34	0.006	190.6	2.28
6.2	0.001=A_{min}	0	0
7.85	0.01	105.44	2.02
8.74	0.012	86.09	1.93
9.82	0.102	8.48	0.93

10.58	0.477	1.01	0.0054
11.28	0.724	0.325	- 0.488
12.07	0.934	0.026	- 1.57
13.47	0.959=A_{max}	0	0

Table 3 allowed us to plot the pH curve as a function of $\left(\log\frac{A-A_{max}}{A_{min}-A}\right)$ (figure 6).

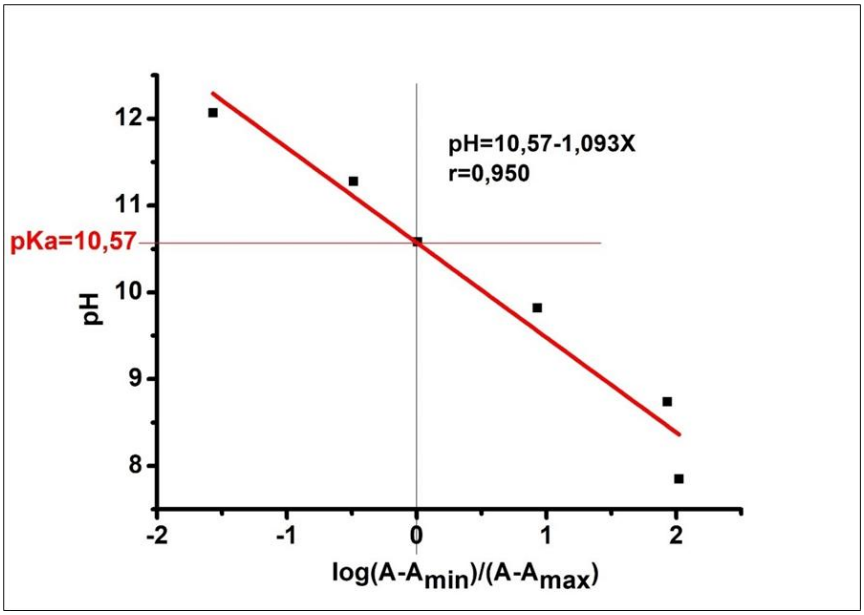

Figure 6: pH as a function of the logarithm of the ratio of concentrations of conjugate species: Linear relationship between pH and $\log\left(\frac{A-A_{max}}{A_{min}-A}\right)$ (λ_{ab}= 278 nm)

This curve yields a straight line with a negative slope and a coefficient of 0.950, close to unity. Analysis of the curve gives a value of 10.57, corresponding to the y-intercept. This value of 10.57 therefore corresponds to that of $pK_A(S_0)$, which is very close to that reported in the literature.

Determination of $pK_A(S_0)$ using the peak λ_{ab}= 222 nm

Figure 2 shows that at a wavelength of 222 nm, the absorbance of the acidic form is low (minimal) and that of the basic form is maximal. Therefore, at this wavelength, we can write:

$$\frac{[R-O^-]}{[R-OH]}=\frac{x}{C_0-x}=\frac{A-A_{max}}{A_{min}-A}$$

As before, we calculated the ratio $\frac{A-A_{max}}{A_{min}-A}$ and the $\log\left(\frac{A-A_{max}}{A_{min}-A}\right)$ as a function of pH.

These values are grouped in Table 4. Next, we plotted $\log\left(\frac{A-A_{max}}{A_{min}-A}\right)$ as a function of pH (Figure 7).

Table 4: Variation of pH as a function of the ratio of concentrations of the basic form to the acidic form

pH	**Absorbance**	$\frac{A-A_{max}}{A_{min}-A}$	$\log\left(\frac{A-A_{max}}{A_{min}-A}\right)$
1.92	0.111	246.4	2.39
2.72	0.096=A_{min}	0	0
3.58	0.106	370.1	2.57
4.34	0.165	52.78	1.72
5.35	0.101	741.2	2.87
6.2	0.103	529.14	2.72
7.85	0.126	122.7	2.09
8.74	0.135	94.15	1.97
9.82	0.504	8.09	0.91
10.58	2.086	0.86	- 0.063
11.28	3.047	0.26	- 0.59
12.07	3.735	0.12	- 0.92
13.47	3.807=A_{max}	0	0

We recall that the equation $pH = pK_A + \log\frac{[Base]}{[Acid]}$ can be written $pH = pK_A + \log\frac{x}{C_0 - x}$ which is equivalent to writing: $pH = pK_A(S_0) + \log\left(\frac{A - A_{max}}{A_{min} - A}\right)$ (Eq-10)

Thus, by plotting the pH curve as a function of $\left(\log\frac{A - A_{max}}{A_{min} - A}\right)$ we obtain a linear correlation with a coefficient of 0.968, a negative slope and an ordinate at the origin equal to $pK_A(S_0)$ =10.65 (figure 7).

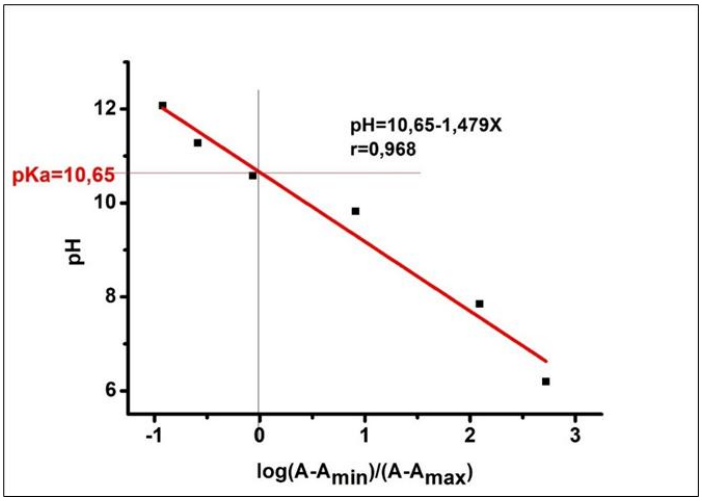

Figure 7: pH variation curve as a function of the logarithm of the ratio of the concentration of the basic form to the acidic form (λ_{ab}= 222 nm)

The two experiments carried out at wavelengths of 278 nm and 222 nm gave pK_A values of 10.57 and 10.65 respectively, with the mean equal to 10.61. These values are very close to those found in the literature [12-14,16].

The pKA values obtained from both methods for each fixed absorption wavelength are grouped together in Table 5.

Tableau 5 : pK_A values obtained in the ground state using the two methods

	λ_{ab}(nm)	pK_A		λ_{ab}(nm)	pK_A	r^2
Méthod I	278 nm	10,60	**Méthod II**	278 nm	10,57	0,950
	222 nm	10,50		222 nm	10,65	0,968
	Moy (pK_A)	**10,55**		Moy (pK_A)	**10,61**	

The two values found from the two methods give an average of 10.55 and 10.61 respectively. Both methods are acceptable, but the former gives an average much closer to that found in the literature.

After determining the $pK_A(S_0)$ in the ground state, it is interesting to determine the $pK_A^*(S_1)$ in the excited state to better understand the reactivity of tyramine between these two states.

Determination Of The Acidity Constant In The Excited State $PK_A^*(S_1)$

The change in electron distribution can therefore lead to other types of chemical reactions in the excited state S_1. This excited state (S_1) has a very short lifetime, from 10^{-11} to 10^{-6} seconds, which makes it difficult to determine its properties. The decay of the excited state can occur through radiative processes or energy transfers. Energy transfer from state S1 to S0 and vice versa proves to be effective for measuring acid-base properties in the ground state (pK_A) and the excited state (pK_A^*) (application of the Förster cycle) [17].

This cycle includes acid-base, spectral, and thermodynamic data. It allows us to determine the pK_A^* (excited state), knowing the pK_A (ground state) after using spectral and thermodynamic data.

After determining the pK_A in the ground state, we still need to calculate the pK_A^* (excited state) using the Förster cycle.

Förster Cycle for the Acid-Base Equilibrium of Tyramine

Three techniques are available to determine acidity or basicity in the excited state.

- Using the Förster cycle based on fluorescence or phosphorescence maxima in highly acidic or highly basic media, as appropriate.
- Using the variation of emission intensity as a function of pH, based on the curve I_f= f(pH).
- Using light photolysis (in this case, the equilibrium constant in the excited state is obtained directly).

For our study, the Förster cycle will be used to determine the $pK_A^*(S_1)$ of the equilibrium:

$$(R-OH)^* \rightleftarrows (R-O^-)^* + H^+ \quad + \quad \Delta H^*$$

Knowing the ground state equilibrium constant $pK_A(S_0)$ of equilibrium :

$$R-OH \rightleftarrows R-O^- + H^+ \quad + \quad \Delta H$$

The FÖRSTER cycle therefore includes spectroscopic and thermodynamic data (Figure 8). To use the FÖRSTER cycle, the deprotonation rate must be higher than the deactivation rate.

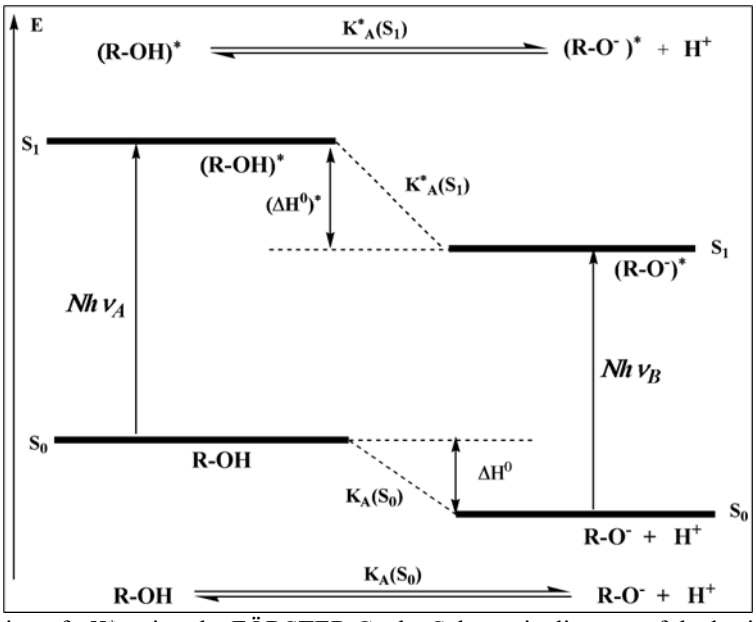

Figure 8: Determination of pK_A^* using the FÖRSTER Cycle: Schematic diagram of the basic and excited energy levels of tyramine

According to the principle of initial and final states, we can write :

$$-\Delta H + \mathcal{N}h\vartheta_A = \mathcal{N}h\vartheta_B - \Delta H^* \quad \Leftrightarrow \quad \Delta H^* - \Delta H = \mathcal{N}h(\vartheta_B - \vartheta_A) \qquad \text{(Eq-11)}$$

With $\vartheta = \frac{c}{\lambda} = c\bar{\upsilon}$

The expression (Eq-11) becomes : $\Delta H^* - \Delta H = \mathcal{N}hc(\bar{\upsilon}_B - \bar{\upsilon}_A)$ (Eq-12)

In this expression:

- $\Delta H^*$and ΔH represent the changes in deprotonation enthalpy in the excited and ground states respectively;
- $\bar{\upsilon}_A$ and $\bar{\upsilon}_B$ represent the wave numbers of the lower-energy absorption peaks of the acid form $(R-OH)$ and the basic form $(R-O^-)$ respectively;
- h is Planck's constant ;
- $\mathcal{N}$ is Avogadro's number;
- c represents the celerity of light.

Furthermore, we know that enthalpy variation (ΔH), free energy (ΔG) and entropy (ΔS) are linked by the relations below:

In the ground state $\Delta H = \Delta G + T\Delta S$ and (Eq-13)

In the excited state $\Delta H^* = \Delta G^* + T\Delta S^*$ (Eq-14)

Expression (Eq-12) becomes $\Longrightarrow \Delta G^* + T\Delta S^* - \Delta G - T\Delta S = \mathcal{N}hc(\bar{\upsilon}_B - \bar{\upsilon}_A)$ (Eq-15)

Assuming that in the ground state and the excited state, the standard deprotonation entropy changes are approximately equal, we can write:

$\Delta G^* - \Delta G = \mathcal{N}hc(\bar{\upsilon}_B - \bar{\upsilon}_A)$ (Eq-16)

In the standard state, we can therefore write: $(\Delta G^0)^* - \Delta G^0 = \mathcal{N}hc(\bar{\upsilon}_B - \bar{\upsilon}_A)$ (Eq-17)

On the other hand, we know that :

$\Delta G = \Delta G^0 + RTlnK_A$ with K_A the acid-base equilibrium constant of the ground-state reaction. However, at equilibrium :

$\Delta G = 0 \Longrightarrow\ 0 = \Delta G^0 + RTlnK_A \ \Leftrightarrow\ \ \Delta G^0 = -RTlnK_A = -2{,}303RT.\log K_A$

Expression (Eq-17) becomes : $2{,}303RT(\log K_A - \log K_A^*) = \mathcal{N}hc(\bar{\upsilon}_B - \bar{\upsilon}_A)$ (Eq-18)

With $pK_A = -\log K_A$ the expression (Eq-18) becomes :

$pK_A^* - pK_A = \dfrac{\mathcal{N}hC}{2{,}303RT}(\bar{\upsilon}_B - \bar{\upsilon}_A)$

With pK_A^* equilibrium acidity constant in the excited state and pK_A acidity constant in the ground state.

In our case we can write: $pK_A^*(S_1) - pK_A(S_0) = \frac{\mathcal{N}hC}{2{,}303RT}(\bar{\upsilon}_B - \bar{\upsilon}_A)$

Hence $pK_A^*(S_1) = pK_A(S_0) + \frac{\mathcal{N}hC}{2{,}303RT}(\bar{\upsilon}_B - \bar{\upsilon}_A)$ (Eq-19)

Thus, replacing $\mathcal{N}, h, C, R$ et T by their numerical value in USI with $T = 298K$ and $\bar{\upsilon}_A$ and $\bar{\upsilon}_B$ expressed in m^{-1} equation (Eq-19) becomes :

$$pK_A^*(S_1) = pK_A(S_0) + \frac{6{,}02.10^{23} \times 6{,}62.10^{-34} \times 3.10^8}{2{,}303 \times 8{,}314 \times 298}(\bar{\upsilon}_B - \bar{\upsilon}_A)$$

$$\Leftrightarrow\ \ pK_A^*(S_1) = pK_A(S_0) + 2{,}0953.10^{-5}(\bar{\upsilon}_B - \bar{\upsilon}_A) \quad \text{(Eq-20)}$$

In general, wavenumbers in spectrometry are expressed in cm^{-1}. In this case, equation Eq-20 can therefore be written as:

$pK_A^*(S_1) = pK_A(S_0) + 2{,}0953.10^{-3}(\bar{\upsilon}_B - \bar{\upsilon}_A)$ (Eq-21)

Application: Numerical calculation of $pK_A^*(S_1)$

Applying equation (Eq-20) and expressing λ in meters (m) after conversion, the values of $pK_A^*(S_1)$ are 4.70 and 4.76 for $pK_A(S_0)$ values of 10.55 and 10.61, respectively.

With a few exceptions, the same value was found between the two methods, thus justifying the reliability and accuracy of both. Based on these results, tyramine tends to be basic in its ground state and acidic in its excited state. Thus, in the excited state, the proton of the (OH) group is more labile than in the ground state. This is likely due to a rearrangement of electrons around the oxygen atom, with a probable deformation of the molecule in the excited state. However, these results are consistent with those found in the literature for phenol. Indeed, for phenols and similar aromatic compounds, the excited pK_A^* of the -OH group is generally lower than the ground-state $pK_A(S_0)$ [18]. Other researchers have found pKa values for the -OH group of tyramine on the order of 10 in the ground state and on the order of 4 to 6 in the excited state [19]. Thus, our pKa values found in the ground state (10.55) and in the excited state (4.70) are very close to those found in the literature [16].

IV. Conclusion

In this study, two methods were used to determine the $pK_A(S_0)$ in the ground state. The first method is based on the variation of the percentage of the acidic or basic form as a function of pH, and the second method uses the Henderson equation. Using the first method, an average value of $pK_A(S_0)$ equal to 10.55 was found; the second method gives a value of $pK_A(S_0)$ equal to 10.61. The small difference between these two values demonstrates the accuracy and precision of both methods.

To further investigate the difference in tyramine reactivity between the ground and excited states, it is also necessary to determine the excited-state acidity constant $pK_A^*(S_1)$. To do this, the FÖRSTER cycle was used to calculate the $pK_A^*(S_1)$ knowing the $pK_A(S_0)$. This cycle resulted in a $pK_A^*(S_1)$ value of 4.7.

Pour ce faire, le cycle FÖRSTER a permis de calculer le $pK_A^*(S_1)$ connaissant le $pK_A(S_0)$. Ce cycle a permis de trouver une valeur de $pK_A^*(S_1)$ égale à 4,7.

The experiment showed that the acidity constant $pK_A(S_0)$ is much higher than $pK_A^*(S_1)$. Thus, in the ground state tyramine tends to be basic, while in the excited state it is rather acidic. In the excited state, the proton of the (OH) group is therefore more labile. This would be due to a new rearrangement of electrons around the oxygen atom, with a probable deformation of tyramine in the excited state.

Références

[1]. Naila, A., Flint, S., Fletcher, G., Bremer, P. & Meerdink, G. (2010). Control Of Biogenic Amines In Food Existing And Emerging Approaches. Journal Of Food Science, 5, R139–R150.

[2]. Linares, D. M., Del Rio, B., Ladero, V., Redruello, B., Martin, M. C., Fernandez, M., & Alvarez, M. A. (2013). The Putrescine Biosynthesis Pathway In Lactococcus Lactis Is Transcriptionally Regulated By Carbon Catabolic Repression, Mediated By Ccpa. International Journal Of Food Microbiology, 165(1), 43–50.

[3]. Alvarez, M., & Moreno-Arribas, V. (2014). The Problem Of Bio Genic Amines In Fermented Foods And The Use Of Potential Biogenic Amine-Degrading Microorganisms As A Solution. Trends In Food Science And Technology, 39, 146–155.

[4]. EFSA Panel On Biological Hazards (2011). Scientific Opinion On Risk Based Control Of Biogenic Amine Formation In Fermented Foods. EFSA Journal, 9, 2393.

[5]. FAO (2014). Assessment And Management Of Seafood Safety And Quality: Current Practices And Emerging Issues. FAO Fisheries And Aquaculture Technical Paper, P. 574.

[6]. European Comission (EC), Commission Regulation No. 2073/2005 Of 15th November 2005 On Microbiological Criteria For Foodstuffs, Official Journal Of European Union, 2005.

[7]. Navarro, J., De Marcos, S. & Galbán, J. (2020). Colorimetric-Enzymatic Determination Of Tyramine By Generation Of Gold Nanoparticles. Microchimica Acta, 187, 174.

[8]. Karovičová, J., Kohajdová, Z. (2005). Biogenic Amines In Food. Chemical Papers, 59, 70-79.

[9]. Papageorgiou, M., Lambropoulou, D., Morrison, C., Kłodzińska, E., Namieśnik, J., Płotka Wasylka., J. (2018). Literature Update Of Analytical Methods For Biogenic Amines Determination In Food And Beverages. Trac Trends In Analytical Chemistry Journal, 98, 128-142. Doi : 10.1016/J.Trac.2017.11.001

[10]. Ordóñez, J., Troncoso, A., García-Parrilla, M., Callejón, R. (2016). Recent Trends In The Determination Of Biogenic Amines In Fermented Beverages–A Review. Analytica Chimica Acta, 939, 10-25. Doi : 10.1016/J.Aca.2016.07.045

[11]. Ndione, P. A., Mbaye, M., Ndione, L., Kital, K., Cissé, L., Sarr, S. O., Fall, D., Coly, A., Gaye-Seye, M. D., Tine, A. (2024). New Method For Analyzing Tyramine By Spectrofluorimetry : Application To Fish. International Journal Of Chemistry, 16 (1), 22-40

[12]. Gloria, M. B. A. (2005). Bioactive Amines. In: H. Hui And F. Sherkat (Eds.). Handbook Of Food Science, Technology And Engineering. London: CRC Press, Pp. 3632.

[13]. Moffat, A. C., Osselton, M. D., Brian, W. (2004). Clarke's Analysis Of Drugs And Poisons, Pharmaceutical Press, London UK.

[14]. Lide, D. R. (1995). CRC Handbook Of Chemistry And Physics: A Ready Reference Book Of Chemical And Physical Data. Boca Raton: CRC Press.

[15]. Vidal Salgado, L. E. Vargas-Hernández C. (2014). Spectrophotometric Determination Of The Pka, Isosbestic Point And Equation Of Absorbance Vs. Ph For A Universal Ph Indicator. American Journal Of Analytical Chemistry, 5, 1290-1301. Doi :10.4236/Ajac.2014.517135

[16]. Mei-Liang, C. C., Devasish, B., Josep, E. R., Juan, P. V., Maria, R. A., And Samuel, C. B. (2011). Determination Of Putrescine And Tyramine In Fish By Micellar Liquid Chromatography With UV Detection Using Direct Injection. The Open Analytical Chemistry Journal, 5, 22-26. Doi: 10.2174/1874065001150100 22

[17]. Sakurovs, R., & Ghiggino, K. P. (1985). Estimation Of Excited State Pk From Rates Of Proton Transfer. Journal Of Photochemistry, 30 (2), 133-140

[18]. Laren, M., Tolbert, K., Solntsev, M. (2002). Excited-State Proton Transfer: From Constrained Systems To "Super" Photoacids To Superfast Proton Transfer. Accounts Of Chemical Research, 35, 19-27

[19]. Giri, S. K., Mohapatra, D. And Tripathi, M. Kr. (2022). UV-Vis Spectroscopic Investigation On Color Change Kinetics Of Lac Dye As Influenced By Some Foods Poilage Metabolites: Validation For Milk Quality Monitoring. Pigment &Resin Technology. Doi: 10.1108/PRT-03-2022-0033